Polymer 169 (2019) 106–114

Contents lists available at ScienceDirect

Polymer

journal homepage: www.elsevier.com/locate/polymer

Ultrafast dynamics of laser from green conjugated-oligomer in solution

Mamduh J. Aljaafreh[a], Saradh Prasad[a,b], Mohamad S. AlSalhi[a,b,*], Zeyad A. Alahmed[a]

[a] Department of Physics and Astronomy, College of Science, King Saud University, 11451, Riyadh, Saudi Arabia
[b] Research Chair on Laser Diagnosis of Cancers, Department of Physics and Astronomy, College of Science, King Saud University, 11451, Riyadh, Saudi Arabia

HIGHLIGHTS

- ASE from the conjugated oligomer (CO) 9,10-Bis[(9-ethyl-3-carbazoyl)-vinylenyl]-anthracene (BECVA).
- BECVA does not produce ASE intrinsically for different solvents in wide range of concentration.
- ASE could be produce only trough energy transfer from one of the efficient CO BECV-DHF.
- The energy transfer process from a macromolecule PFO to BECVA was not efficient.
- The TRS studies demonstrated that BECVA begins the emission before the donor (BECV-DHF), even at low concentrations.

ARTICLE INFO

Keywords:
Amplified spontaneous emission
Energy transfer
Absorption
Fluorescence
Conjugated oligomer BECVA

ABSTRACT

In this work, we report on the time resolved spectroscopy of amplified spontaneous emission (ASE) from the conjugated oligomer (CO) 9,10-Bis[(9-ethyl-3-carbazoyl)-vinylenyl]-anthracene (BECVA) only upon energy transfer from another oligomer 1,4-Bis(9-ethyl-3-carbazo-vinylene)-9,9-dihexyl-fluorene (BECV-DHF). BECVA do not dissolve readily in tetrahydrofuran (THF) at room temperature, but completely dissolved when the temperature of the solution (THF & BECVA mix) was risen to 65 °C and remained dissolved even after cooling to room temperature. The process of heating and dissolving do not affect the performance of the CO. The heat-treated solutions were used to perform all experiments, unless mentioned. The absorption spectra indicated no aggregate formation upon increasing concentration, but the fluorescence spectra were very different for several concentrations of the solution, indicating the presence of the ***excimer.*** Pure BECVA in THF was pumped at various pump powers and concentrations. This produced only a broadband emission (from 500 to 750 nm) with a FWHM of 250 nm, which has potential applications in white light OLED. Next, we tried to produce ASE using the energy transfer process from a conjugated polymer (CP) poly (9,9-dioctylfluorenyl-2, 7-diyl) (PFO); however, this did not produce ASE, which could be due to the significant hindrance of the macromolecular PFO. The intensity of the BECVA spectra was enhanced with energy transform from PFO. The output was a broadband emission ranging from 400 to 750 nm (FWHM 350 nm). Finally, we added the oligomer BECV-DHF in solution (THF) to the BECVA solution at optimal pump power and concentration of donor (BECV-DHF), and the super-irradiant laser was produced from BECVA at 500 nm with a FWHM of 6 nm. The ultrafast dynamics of the BECVA solution under high pump power excitation and different energy donor (PFO and BECV-DHF) were extensively studied in this work. To the best of our knowledge, this is the first report of a CO that does not intrinsically produce ASE, but produces efficient ASE only via the energy transfer process by another CO.

1. Introduction

In our everyday life, laser is a crucial device with wide range of applications [1,2] especially in technology [3], spectroscopy [4–6], and science [7], medical [6,8], and optical communications [9,10].

Organic CPs and COs have emerged as attractive materials in recent years. These materials have a great role in the development of inexpensive and multi-use optoelectronic devices on large-scale substrates. In addition, the CP and CO have extraordinary optical and physical properties such as high optical gain and a tunable wide range of emission spectra. High fluorescence quantum yield [11,12] triggered a revolution in many fields such as light-emitting diodes [13–15], and

* Corresponding author. Department of Physics and Astronomy, College of Science, King Saud University, 11451, Riyadh, Saudi Arabia.
E-mail addresses: maljaafreh@ksu.edu.sa (M.J. Aljaafreh), srajendra@ksu.edu.sa (S. Prasad), malsalhi@ksu.edu.sa (M.S. AlSalhi), zalahmed@ksu.edu.sa (Z.A. Alahmed).

https://doi.org/10.1016/j.polymer.2019.02.022
Received 19 November 2018; Received in revised form 7 February 2019; Accepted 10 February 2019
Available online 26 February 2019
0032-3861/

photovoltaics [16] as well as non-linear optics [17,18]. Moreover, these materials have inspired intense and abundant research in areas such as laser media [19–22].

In contrast to the CP, the CO consists of a limited and fixed number of repeating monomer units. Moreover, they have priority, especially in the easier purification process, a specified molecular weight, and better control of molecular structures. However, in the laser action, it could be seen that oligomers possess the advantages of conventional dyes and also conjugated polymer [23,24] as these small molecules have features that look like laser dyes and conjugated polymers.

CPs and COs have gained prominent attention as materials for producing ASE, the prelude of lasing action. ASE is a type of mirrorless semi-coherent laser with no feedback process [25]. Many studies have reported producing ASE in a very broad range of conjugated polymers and oligomers using optically pumped excitation. Notably, for any active media producing laser, it is not necessary to produce ASE, while the reverse is correct [26]. ASE was first presented from a liquid solution of a CP (MEH-PPV) by Moses et al. [14]. Musubu et al. demonstrated a self-waveguided single crystal thiophene/phenylene co-oligomer [α, w-bis-biphenyl-4-yl-terthiophene] that showed laser oscillation when the crystals worked as an optical cavity [27]. The ASE of the crystals of the thiophene/phenylene co-oligomer was observed at both room temperature and low temperatures in a single crystal at room and low temperatures under the intense excitation. Two bands took place in the vibronic sidebands with highly polarized optical gains of 50 cm^{-1}. Optically pumped lasing at room temperature was obtained for a molecular crystal of 2,5-bis(4′-cyanobiphenyl-4-yl)thiophene (BP1T-CN) [28]. ASE and blue fluorescence were observed when the single crystal of p-sexiphenyl (p-6P) was pumped by UV excitation [29].

Förster resonance energy transfer (FRET) phenomena have a crucial and wide application in biophysics and chemistry from mesoscopic to molecular systems. FRET considers the non-radiative transfer of energy from a donor molecule to the acceptor molecule, and includes the long-range coupling of acceptor and donor dipoles. The FRET equation has been successfully applied to explain the energy transfer phenomenon in polymer blend systems [30,31] and molecular dye systems [32,33]. The occurrence of the FRET depends on many key parameters. One is the distance between the donor and acceptor, which should be in the range of 10–100 Å (Angstrom), whereas the second condition that needs to be achieved is the overlap between the emission spectra of the donor and absorption spectra of the acceptor molecules [34,35]. It is critical to understand the physics of an exciton transfer from a donor to an acceptor to achieve better photovoltaic materials and also design high performance optoelectric devices including OLEDs [36] and laser devices [37].

In this work, we investigated the spectral properties of the CO BECVA in the THF under pulsed laser excitation using the energy transfer process. The results showed that under sufficient concentration and ideal pump power, BECVA could exhibit ASE at 500 nm in the mixtures of BECV-DHF as the donor and BECVA as the acceptor with a FWHM of 6 nm and divergence of 10 mrad. Time resolved dynamic studies showed that fluorescence from the donor always appeared later (around 1 s).

2. Materials and methods

The CO BECVA and BECV-DHF oligomer with molecular masses of 616.81 g mol^{-1} and 773.12 g mol^{-1} respectively. The CP PFO had the number-average molecular weight (Mw) of 95,000 ± 45,000 g mol^{-1}, and the PDI (polydispersity index) = 2.6 [38]. The above materials were sourced from the American Dye Source (Montreal, Quebec, Canada) and used as received. The molecular structures of the oligomers and PFO polymer are shown in Fig. 1. A polished quartz cuvette with the dimensions 1 cm × 1 cm × 4 cm and an optical path length of 10 mm was used to measure the spectra and laser properties of the solutions of these materials as stated before. THF (spectroscopic grade, 99.8% purity) in a wide range of concentrations (1–810 μM) was used as the solvent for both COs and PFO. All experiments were conducted at room temperature (20 °C). The experiments were also carried out in different solvents such as benzene, THF, toluene, and Chloroform. But the efficiency of energy transfers to CO BECVA from BECV-DHF and PFO was better in THF than other solvents. Absorption spectra were obtained by exciting the sample at a 355 nm excitation wavelength and the emission spectra in the 330–550 nm range was recorded by using a Perkin-Elmer Lambda 950 spectrophotometer (Llantrisant, United Kingdom). Additionally, by using the same excitation wavelength (355 nm), the fluorescence spectra were obtained in the 380–700 nm range with a Perkin-Elmer LS-55 spectrofluorometer.

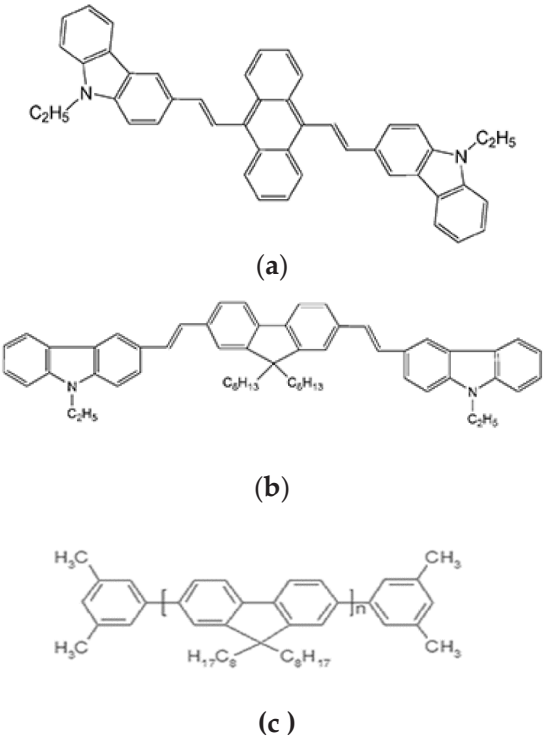

Fig. 1. Molecular structure of the COs and CP: (**a**) BECVA, (**b**) BECV-DHF, and (**c**) CP PFO.

The excitation laser was the third harmonic of an Nd:YAG laser (Les Ulis, France) with a wavelength of 355 nm, pulse duration of 10 ns, and repetition rate of 10 Hz, which was used to measure the ASE. A quartz plano-convex lens with a 5 cm focal length was applied to focus the UV laser pulse into the liquid solution stored in the cuvette, and successfully made the transverse excitation to the samples. At the optimum experimental conditions such as concentration, the same cuvette, and pump energy, the experimental results showing that the superradiant emission ranging from LIF to ASE was fed to a fiber optic cable that was connected to the spectrometer. A Gentec Maestro power energy meter (Quebec, Canada) was utilized to measure the output power of the ASE.

3. Results and discussion

3.1. Dynamic light scattering of oligomer (DLS)

When 650 μM of the CO BECVA, as 2 mg, was dissolved in 4 mL of THF, the resulting solution was very murky. The solution was kept in an encapsulated test tube and submersed in a hot water bath at 65 °C for 3 min. Then, the solution became homogenous and clear. The DLS experiment was done for both the unheated and heated sample. For the unheated sample (Fig. 2i), the size distribution was around 1560 nm–3050 nm with an average size of ~2170 nm, where around 63% of aggregates were in the size range of 2000 nm–2300 nm. On the

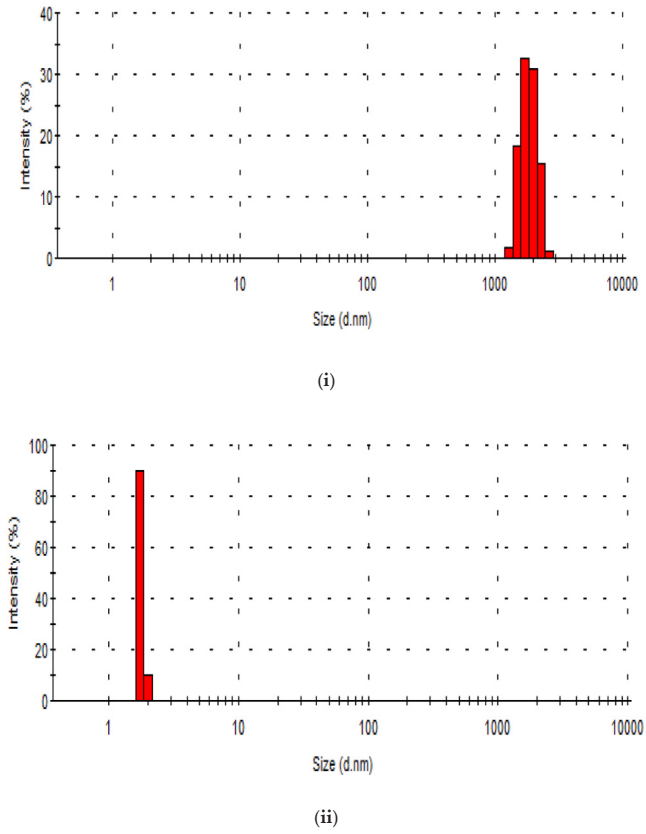

Fig. 2. The DLS size distribution of the CO BECVA (**i**) before, and (**ii**) after heat treatment.

other hand, the heated sample (Fig. 2ii) had a size distribution of only ~3.5 nm for about 90% of the particles in the solution. Due to the high solubility of BECVA upon heating, the oligomers were homogenously dissolved in the solution, which made the DLS experiments very difficult. However, the unheated sample showed that the CO had a large aggregation that was eliminated by thermal agitation.

3.2. Absorption and fluorescence properties

Fig. 3 shows the absorption spectra of the BECVA dissolved in THF at different concentrations ranging from 40 μM to 10 μM, which represented an absorption band around 425 nm and a shoulder in the UV-region. When the concentration was increased, we did not find a new absorption peak in the longer wavelength region of the absorption spectra. Only the optical density of the band around 425 nm increased, but the absorption profile remained unchanged as the concentration was increased. Note that the optical density shown in Fig. 3 is not to scale. In our previous article, we were able to show that the CP PFO could exhibit a dimer state at high concentration and manifested as a new absorption peak at a longer wavelength (425 nm) than the primary band (355 nm) [39]. Nevertheless, in the case of BECVA, there was no dimer formation.

The fluorescence spectra of BECVA in a solution of THF at different concentrations (810 μM–12 μM) were obtained as shown in Fig. 4. At a low concentration (25 μM), the fluorescence spectrum curve showed the emission peak of BECVA in the blue region with broad emission bands centered at 495 nm. At a concentration of 50 μM, the peak shifted to 510 nm. Further increasing the concentration to 100 μM shifted the peak to 525 nm. When the concentration was further increased in steps (from 200 μM to 404 μM), the peak red shifted to 540 nm, then 550 nm. This phenomenon could be attributed to the reabsorption process; particularly for this CO, the reabsorption was very high, which reduced the quantum yield. Note that the peak around 710 nm was due to the second order scattering of the excitation wavelength (355 nm) from the grating of the monochromatic light of the spectrofluorometer.

3.3. Laser induced fluorescence (LIF)

To study the spectral profile of the laser-induced fluorescence (LIF) of the CO BECVA under high power excitation, BECVA was dissolved in THF at various concentrations. With the concentration fixed at 100 μM, the excitation source was an UV laser at 355 nm that transversely excited the solution. At a pump power of 20 mJ, the LIF spectrum was collected using an ultrafast Si photodetector (UPD) and recorded via fiber using an ocean optics spectrometer.

For the high concentration, the spectral FWHM was around 250 nm with a peak around 570 nm. For the low concentration, as shown in Fig. 5, the LIF spectra showed a narrower spectral profile with a FWHM of 100 nm with two distinct peaks around 500 nm and 550 nm for the same pump power. Moreover, the LIF spectra also indicated that BECVA existed in both a monomer and excited state in the THF solution. Due to the high pump power from the laser excitation, the LIF produced by CO was narrower than the steady state excitation by the spectrofluorometer. The blue shift showed that for the extremely low concentration, the reabsorption became very low so the spectra became narrow. For a wide range of concentrations (810 μM–12 μM) and high pump power, this oligomer produced only LIF and did not produce ASE on its own.

3.3.1. Energy transfer between the CP PFO and CO BECVA

Since BECVA does not produce a laser on its own, we tried to employ energy transfer between PFO (donor) and BECVA (acceptor). Fig. 6 shows that the overlap between the fluorescence of the donor, and absorption of the oligomer (acceptor) was about 100%.

The energy transfer experiment was conducted using transfer pumping. The starting solution was the polymer PFO at a concentration of 20 μM, half filled in a cuvette (2 mL) before adding the oligomer BECVA at a concentration of 100 μM drop by drop (each drop was 0.5 mL). The intensity from PFO started to reduce and a broad patch of emission with a broad band ranging from 500 to 700 nm appeared when the concentration of the donor was 16 μM and the acceptor was 160 μM. Furthermore, when the concentration of the acceptor was increased, the emission from PFO diminished and that from BECVA improved. Fig. 7 shows the time resolved spectra of this process for a fixed concentration of the donor (10 μM) and acceptor (270 μM). The spectra were recorded with an interval of 500 ps (0.5 ns) for a duration of 50 ns. However, the figure only shows the range close to the event (energy transfer process).

The Förster transfer radius (R^0) is known as a critical transfer distance. The rate of energy transfer depends on its value being about 10 nm or less. R^0 is proportional to the spectral overlap of the emission (donor) and the absorption of the acceptor. When the intermolecular separation is less than or equal to R^0, the acceptor molecules will compete well with all other decay routes. R^0 can be calculated using the following equation [40,41]:

$$R_0^6 = \frac{9000\,(\ln 10)\,k^2 \varnothing_D}{128\,\pi^5 n^4 N_0} \int \frac{F_D(\bar{\upsilon})\varepsilon_A(\bar{\upsilon})\,d\bar{\upsilon}}{\bar{\upsilon}^4} \quad (1)$$

where k is the orientation factor; $\varepsilon_A(\bar{\upsilon})$ is the molar extinction coefficient (EC) of the acceptor that is wavelength dependent; n corresponds to the refractive index of the solvent; $\varnothing_D$ is the QY of the donor; $F_D(\bar{\upsilon})$ is the spectral distribution of the donor normalized to unity; $\bar{\upsilon}$ is the wave number; and N_0 is Avogadro's number.

The excitation coefficient of the acceptor was $6.03 \times 10^4\ M^{-1}cm^{-1}$, n for the THF was 1.407 at 20 °C, k^2 for the homogenous solution was $(\frac{2}{3})$, and the QY of the donor (PFO) was calculated to be 0.6 [42]. Hence, the R_0 = 49.45 Å.

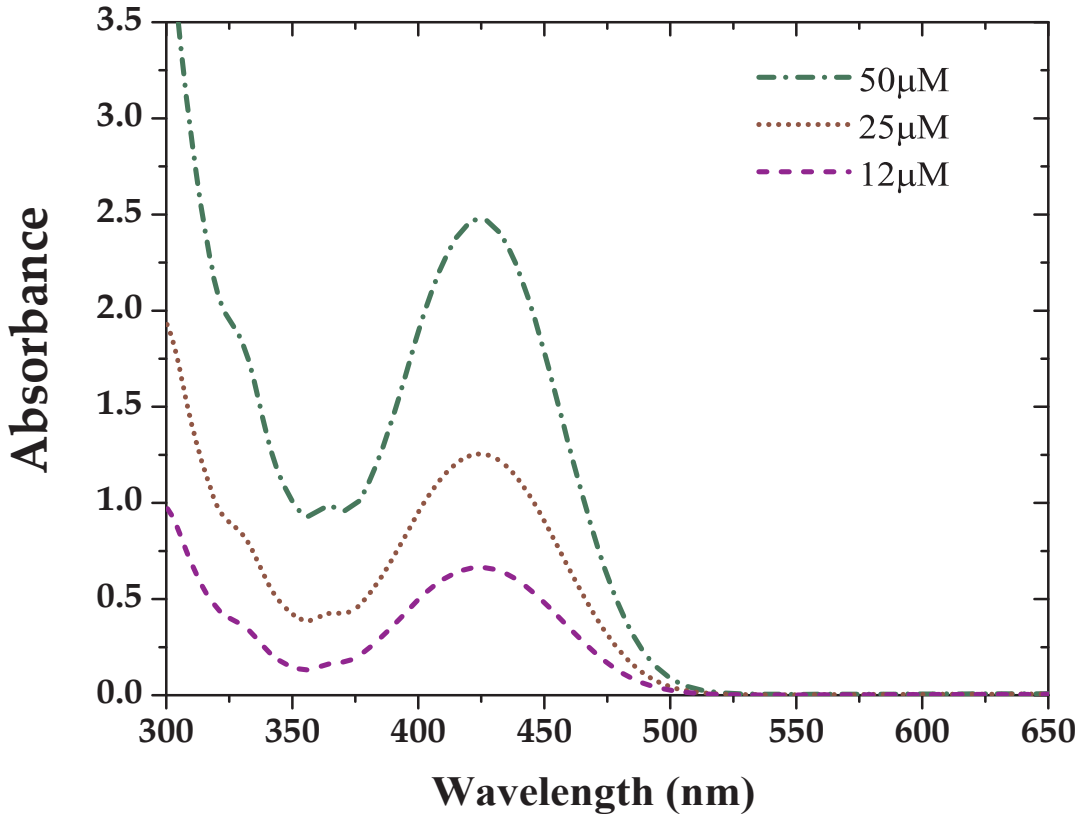

Fig. 3. Absorption spectra of the CO BECVA in THF for different concentrations.

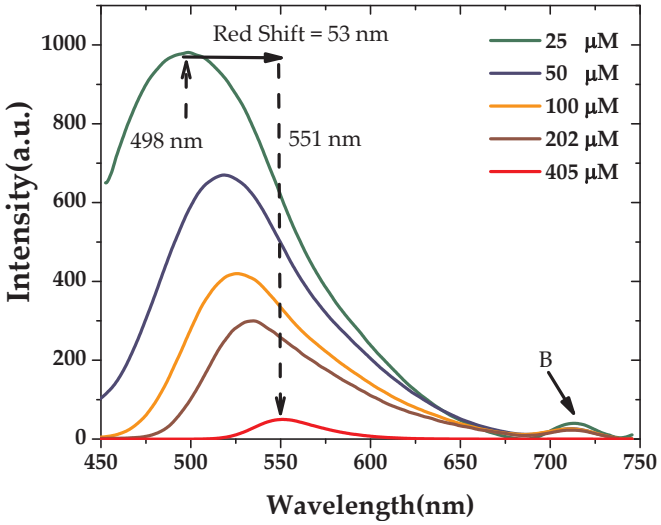

Fig. 4. Fluorescence spectra of the BECVA in THF in different concentrations. The fluorescence peak is at 488 nm for a concentration 25 μM and shifts towards red for increase in concentration, (B) the peaks are due second order diffraction (Rayleigh) scattering of excitation wavelength 355 nm.

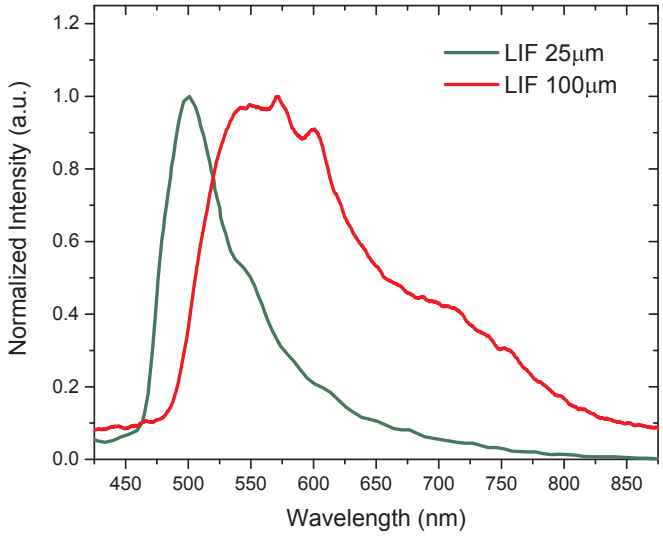

Fig. 5. LIF of the CO BECVA at high (100 μM) and low concentration (25 μM) for a pump power of 20 mJ.

According to Fig. 7, the spectrum had a wide range that started at 400 nm and cut off at 600 nm due to the grating selection; the actual fluorescence band from the CO BECVA extended beyond 600 nm up to 740 nm. The figure shows that at the beginning, the CO started the emission with little emission from PFO, and the trend was continuous for the entire duration of the excitation. The spectra show four peaks at 420 nm and 445 nm from PFO, and 476 nm and 500 nm corresponded to the peak of the CO BECVA. These peaks appeared at high pump power, and could be attributed to the monomeric and excimeric state of the CO, respectively. The excimer could be formed even with steady state excitations. In order to obtain the ASE from the CO, several different combinations of pump power, concentration ratio of donor to acceptor in the solution, and different solutions were tested, but the ASE from the CO was not active using energy transfer from PFO. However, this solution produced a near white light-like fluorescence that could potentially be useful for designing new OLEDs. Note that the spike at 532 nm was due to the second harmonic residual from the pump laser. Even if all necessary conditions were met for energy transfer, it did not occur, which could be because PFO is a large macromolecule and the CO was not able to come close due to significant hindrance.

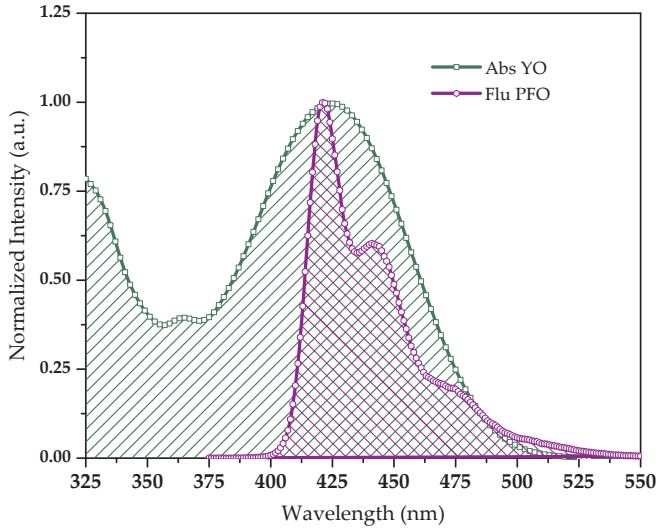

Fig. 6. The spectral overlap between the fluorescence spectrum of PFO and the absorption spectrum of BECVA.

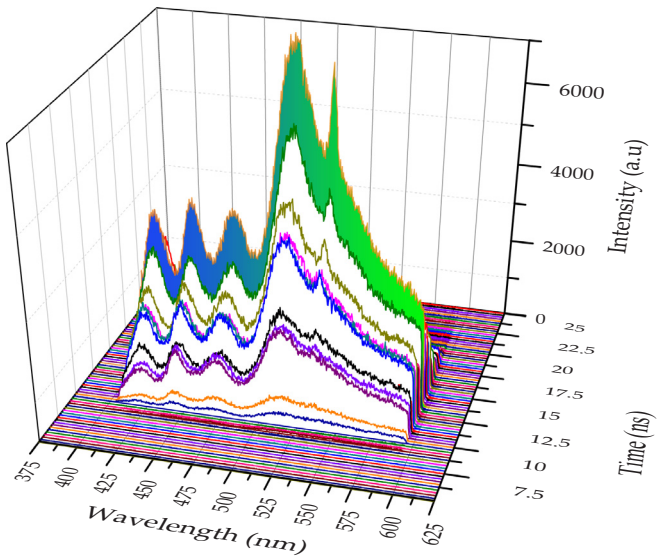

Fig. 7. Time evolution of the energy transfer process between PFO and BECVA.

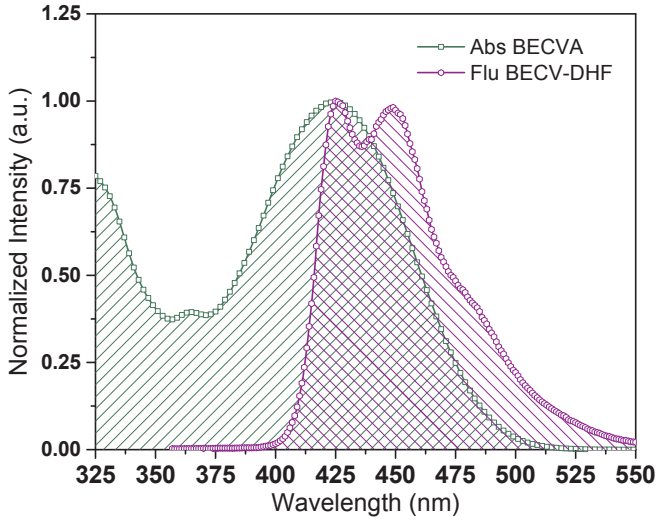

Fig. 8. The spectral overlap between the fluorescence spectrum of BECV-DHF (81 μM) and the absorption spectrum of BECVA (50 μM).

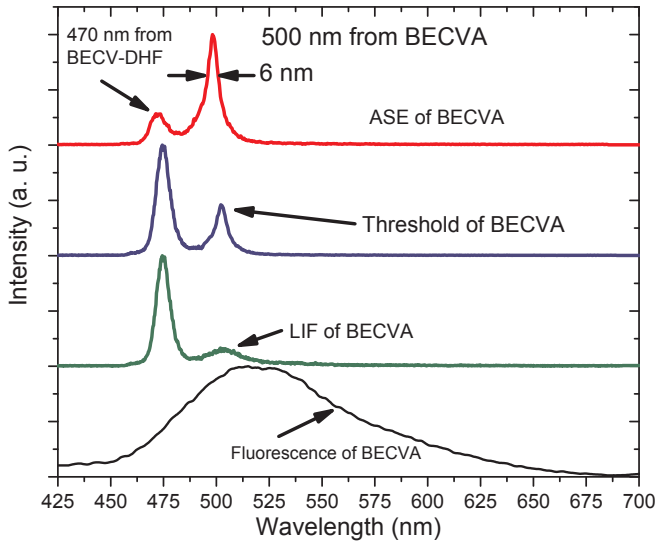

Fig. 9a. The fluorescence, LIF, threshold, and ASE from BECVA via the energy transfer of the CO BECV-DHF.

3.3.2. *Energy transfer between the COs BECV-DHF and BECVA*

In order to increase the chance of achieving an ASE (if any) output from the CO BECVA, we employed an energy transfer technique of two COs (BECV-DHF and BECVA). COs have a smaller number of iterating monomer units (3–10) and are transitional between a monomer and a polymer. Only a few COs produce efficient lasers [17,24,43], and can be used as energy donors for other laser media; herein, the BECV-DHF oligomer was employed for this purpose. Fig. 8 shows the overlap between the fluorescence spectrum of BECV-DHF and the absorption spectrum of BECVA. The overlap between the oligomers BECV-DHF and BECVA was about 87%, indicating that BECVA could represent a good energy donor for the BECVA acceptor.

Fig. 9 shows the fluorescence of BECVA when the concentration was 160 μM. When the concentration of BECVA-DHF was 520 μM, 0.5 mL of BECVA was added to that solution, and BECVA-DHF produced a very narrow peak at 470 nm with a FWHM of 15 nm. The CO BECVA produced LIF with a FWHM at 30 nm and 500 nm, respectively. When the concentration of BECVA-DHF was 433 μM and BECVA was 270 μM, the peak at 500 nm became a spectrally (15 nm of FWHM) and spatially (divergence of 10 mrad) narrow cone of light (green). Note that this was the minimum pump power (20 mJ) and the concentration required for producing the threshold ASE. When the concentration donor oligomer was 324 μM and the acceptor concentration was around 405 μM, the ASE from the CO BECVA was obtained with a peak at 500 nm, a FWHM of 6 nm and 8 mrad (Fig. 9b).

Fig. 9c shows the time evolution of the LIF with a smooth sharp cone, which had a pulse width of only 4.35 ns from the CO BECVA samples described earlier in Fig. 8a. The LIF was transformed into the threshold ASE with collimation (from 4π to 10 mrad), spectral narrowing (from 100 nm to 6 nm), and temporal narrowing (from 4.35 ns to 0.890 ns), showing a strong interaction between photons and inversion. As it increased, the concentration of the BEVCA ASE was obtained with a smooth sharp pulse of 0.91 ns (FWHM). These are the two characteristic manifestations of the stimulated emission dominating over the spontaneous emission with the onset of the ASE.

The energy transfer experiment between the oligomers was done through exactly the same procedure as stated above, but the PFO was replaced with the CO BECV-DHF. The concentration of BEVC-DHF was 520 μM and BECVA was 160 μM. When the concentration of BEVC-DHF was 433 μM and BECVA was 270 μM in the solution, the ASE intensity

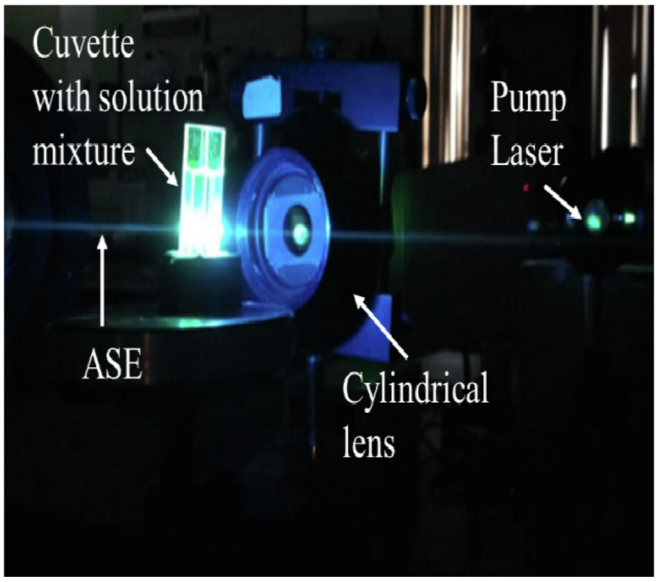

Fig. 9b. Photograph of the ASE from a mixed solution of the COs BECVA and BECV-DHF.

from BEVC-DHF was reduced and the intensity of BECVA started to appear. We observed an efficient energy transfer because the overlap between the two oligomers was very large and the calculated critical distance (R_0) was 51.79 Å [Förster transfer radius (R_0)]. Since the excitation coefficient of the acceptor was $6.39 \times 10^4\, M^{-1}cm^{-1}$, the refractive index of THF was 1.407 at 20 °C, the dipole orientation factor for a homogenous solution was ($\frac{2}{3}$), and the QY of the donor (blue CO) was calculated to be 0.8612.

3.4. Time evolution of energy transfer between the COs BECV-DHF and BECVA

The time resolved dynamics of the energy transfer process between the two COs in solution was measured using a picosecond camera, and the pump source was the third harmonic of the Nd:YAG nanosecond laser. Initially, the oligomer (donor, BECV-DHF) solution with a concentration of 650 μM (2 mL in volume) was kept in a quartz cuvette. The acceptor (BECVA) was added in drops of 0.5 mL.

This figure can be seen as evidence and verification of the occurrence of the external energy transfer from the donor to the acceptor. The mixture was pumped using the third harmonic of the Nd:YAG laser, the pump power was 18 mJ; i.e., under the same operation conditions. Even though the concentration of BECVA was very low, the fluorescence from it started prior due to the highly efficient resonant energy transfer from the CO BECV-DHF. In FRET process, donor transfers the energy to acceptor trough a non-radiative dipole-dipole induction process (dipole antenna, similar to the wireless charges to the mobile phones) due to the electric field produced by polarization of molecules under excited state. This reduces the excited state life time of the donor (CO BECV-DHF in our case). But the acceptor could be excited directly from the pump (incoming photons), in addition it could also excited by FERT, this increases the life time of the acceptor (BECVA) [44]. For the above described experimental conditions, the fluorescence of acceptor starts 2.0 ns earlier. However, due to the high photo flux (from pump pulse) available to the already efficient donor (BECV-DHF), it took over to produce fluorescence and ASE in a sequential manner. The donor rise and falls at rapidly rate than acceptor. The result showed the ASE peaks, where one was around 465 nm, which corresponded to the CO BECV-DHF which dominated, and the other was a small signal around 500 nm due to BECVA, with a narrow spectral bandwidth at 35 nm (FWHM) (narrow when compared to the LIF FWHM of 100 nm), which was a very good indication that the BECVA oligomer could produce ASE under unique conditions.

When the solution was pumped with an energy of 25 mJ and the concentration of donors and acceptors was 371 μM and 347 μM,

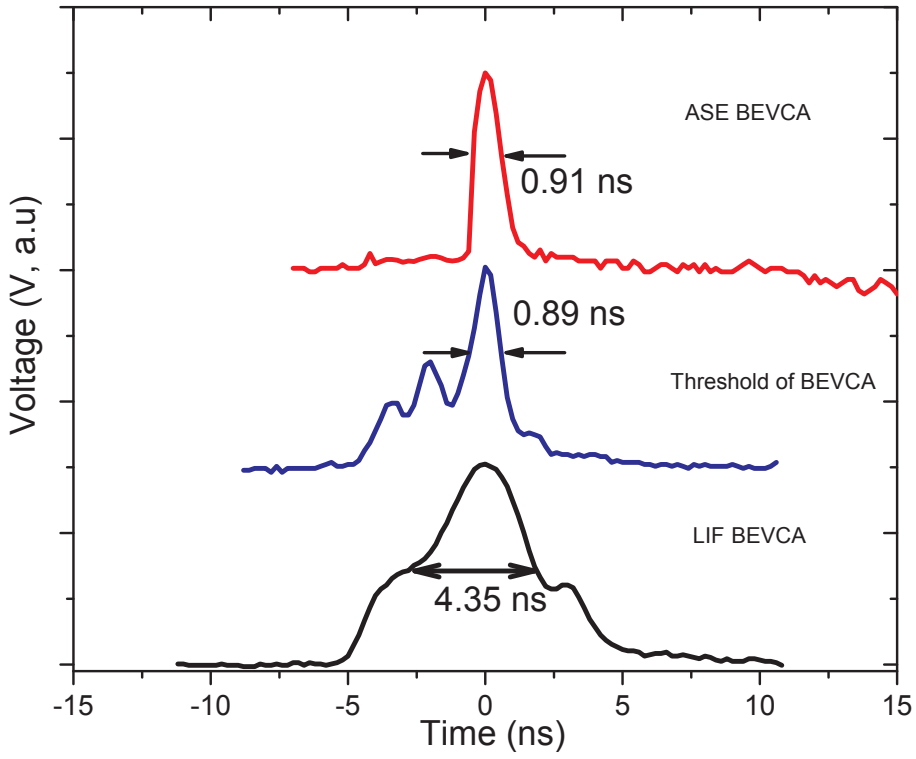

Fig. 9c. The LIF, threshold, and ASE from the CO BECVA via the energy transfer of the CO BECV-DHF in the time domain using a digital oscilloscope.

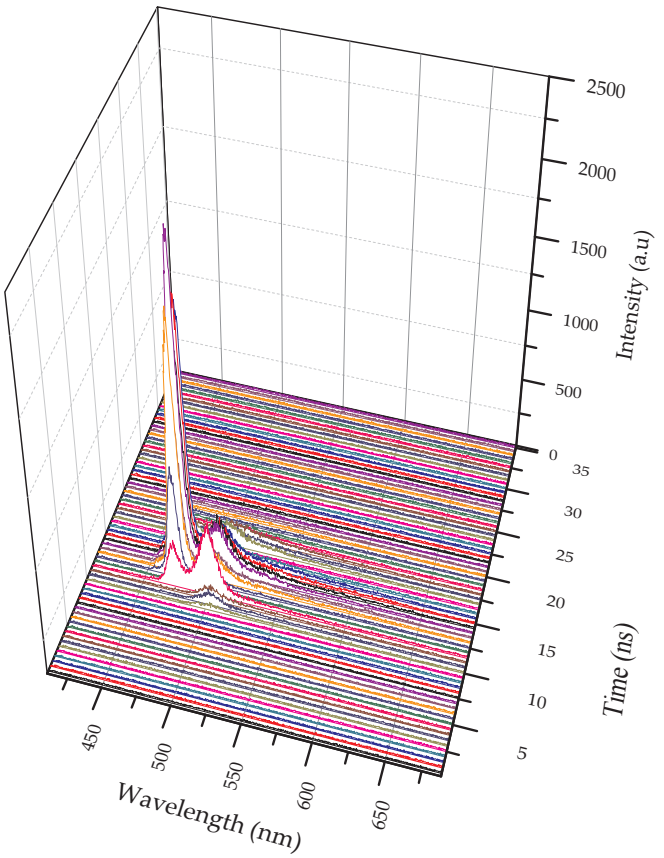

Fig. 10a. The dynamics of the energy transfer process when the concentrations of the donor (BECV-DHF) and acceptor BECVA were 520 μM and 160 μM respectively, and the pump energy was 18 mJ.

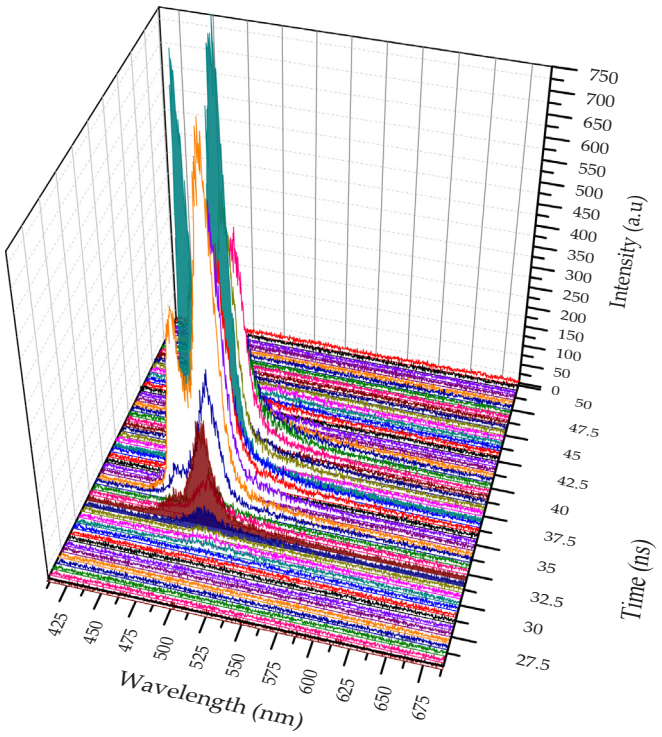

Fig. 10b. The dynamics of the energy transfer process when the concentration of the donor (BECV-DHF) was 371 μM and 347 μM, and the pump energy was 25 mJ.

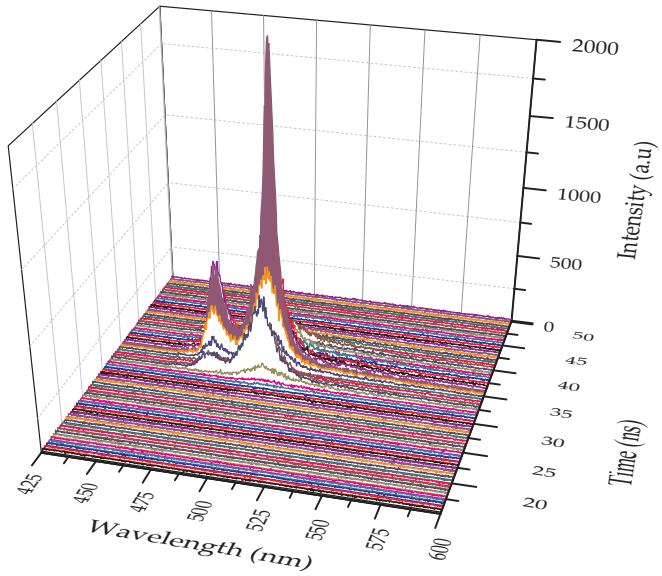

Fig. 10c. The dynamics of the energy transfer process when the concentration of the donor (BECV-DHF) was 324 μM and 405 μM, and the pump energy was 25 mJ.

respectively, the acceptor started to fluoresce first (violet line at 30.5 ns), then after 1 ns (immediately), the spectral narrowing took place and the FWHM was about 15 nm (blue line at 31.5). At this point in time, the donor was barely able to produce fluorescence. However, the donor was inherently efficient and produced ASE after 3 ns of fluorescence along with the acceptor (orange line at 33 ns). The FWHM of the donor was 6 nm and that of the acceptor was 10 nm. Part of the energy (photo flux from the pump) was transferred to the acceptor and the rest produced an ASE from the donor itself; therefore, there could be competition between the donor and acceptor under a high population inversion (PI) state. Hence, the intensity of both became comparable. The spectral narrowing was also complemented by a spatial narrowing of a green strip of light with a divergence of 10 mrad.

Fig. 10c shows the strong ASE at 500 nm due to the increase in the number of CO BECVA molecules, so the ratio between the peaks' intensities was 7 to 1. The result showed that there was one ASE band around 500 nm, which coincided with the fluorescence peak of BECVA, and the ASE peak around 470 nm was weak, as shown in Fig. 10c. The energy transfer always favored the longer wavelengths to emit first. The fluorescence of BECVA started at 33 ns, but the fluorescence from BECV-DHF only appeared after 1.5 ns. At this concentration, the energy transfer was so efficient that BECVA produced ASE in 3 ns from the time of fluorescence, but the peak at 470 nm was due to the BECV-DHA donor growing only as the LIF with a FWHM of 40 nm, while the acceptor FWHM was 7 nm.

Fig. 11 shows that all of the energy transfer from the donor to the acceptor indicated a strong confirmation of the energy transfer process. There was only one peak at 500 nm that corresponded to the CO BECVA, while the other peak from BECV-DHF was completely absent, which shows that the energy transfer was very efficient for this combination of donor and acceptor oligomers.

4. Energy transfer mechanism in the COs

When a molecule in a ground state is excited by the incoming photon to an excited state, it becomes polarized. These molecules stay in an excited state for few nanoseconds. If a suitable acceptor molecule with a critical Förster radius (≤ 10 nm) is present nearby, then there is a high probability that energy transfer will occur resonantly [37,45], which is called the Förster-type resonant energy transfer. This process is

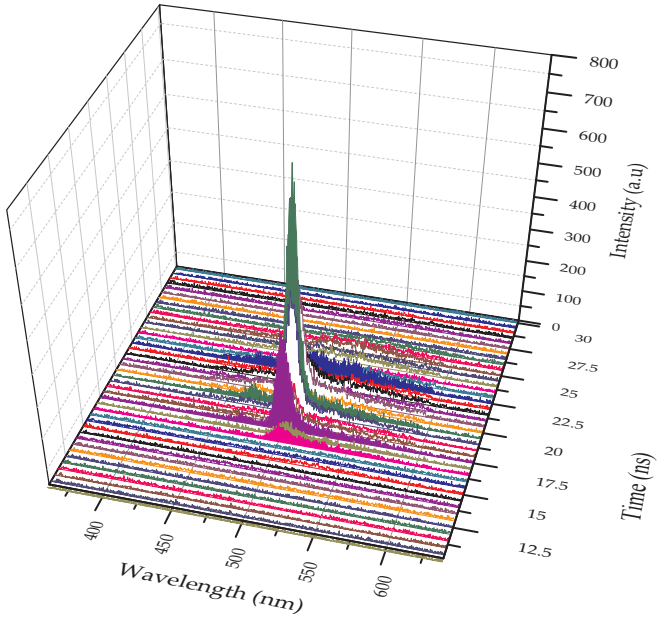

Fig. 11. The dynamics of the energy transfer process when the concentration of the donor (BECV-DHF) was 288 μM and 540 μM, and the pump energy was 25 mJ.

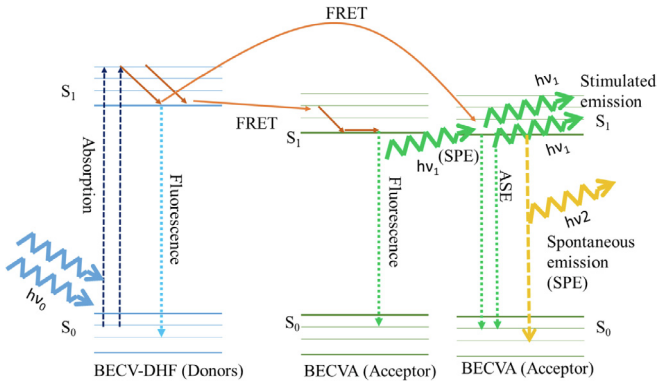

Fig. 12. The energy transfer between the COs BECV-DHF(donor) and BECVA (acceptor).

useful in finding the underlying mechanism of various chemical and biological processes [46]. Fig. 12 shows an incident photon of higher energy (3.49 eV, pulse energy 25 mJ) with a large photon flux (8.96×10^{15} photon/ns). The molecules of the CO BECV-DHF—the donor—in ground state (S_0) get excited to state (S_1). Now, the excited BECV-DHF has several ways to come back to the ground state. First, by producing fluorescence. Second, by non-radiative decay, and third by transferring energy to the acceptor. BECVA was excited via resonance energy transfer. The acceptor could decay by producing a photon of energy, $h\nu_1$, (spontaneous emission). If BECVA is under the PI condition, the spontaneous emission emits a photon that interacts with other oligomers in an excited state to produce a photon $h\nu_1$ by the stimulated emission process. Which leads to the amplification of spontaneously emitted photon and a mirrorless laser is possible from the large optical gain in a single pass.

From our experiment and under all concentrations, the acceptor began to produce fluorescence even though the donor started absorption later and was rapidly absorbed to produce PI conditions (for the donor). These excited donors transferred the energy almost instantaneously (fs). Therefore, the CO BECVA (acceptor) was able to form the PI and hence produce the ASE.

5. Conclusions

The spectral and laser properties of a new CO BECVA with a broad range of emission from 500 to 7500 nm in THF were reported. Absorption, fluorescence, and the ASE characteristics were studied when the oligomer was excited with a tripled frequency Nd:Yag laser. The results showed that BECVA could not produce ASE by itself even at the maximum power and with different concentrations. The energy transfer from PFO also did not work because of the significant hindrance of the macromolecules. However, success was achieved via the energy transfer process from another CO BECV-DHF that emitted in the blue region, and since the conditions for energy transfer were achieved, a superradiant emission from BECVA at a wavelength of 500 nm and a 6 nm spectral width was produced. Furthermore, the time evolution of the energy transfer in the CO solutions was studied. The TRS studies demonstrated that BECVA begins the emission before the donor, even at low concentrations. Therefore, BECV-DHF is a very good material that produces PI quickly, and forces the acceptor CO BECVA to produce ASE.

Author contributions

Mohamad S. AlSalhi and Zeyad A. Alahmed conceived the idea and planed the work; Mamduh J. Aljaafreh Saradh Prasad did spectral and laser studies of the materials; Saradh Prasad and Mamduh J. Aljaafreh, analyzed the data as well as explained the results and wrote the manuscript.; Mohamad S. AlSalhi and Zeyad A. Alahmed reviewed and edited the manuscript.

Acknowledgments

The authors are grateful to the Deanship of Scientific Research, King Saud University for funding through Vice Deanship of Scientific Research Chairs.

References

[1] A.-K.I. Zuhaier, K. Mohammad, S. Devanesan, M.S. AlSalhi, S. Prasad, V. Masilamani, Shelf-life enhancement of donor blood by he–ne laser biostimulation, Curr. Sci. 109 (2015) 1151.
[2] D.H. Sliney, The development of laser safety criteria—biological considerations, Laser Applications in Medicine and Biology, Springer, 1971, pp. 163–238.
[3] R. Paschotta, Encyclopedia of Laser Physics and Technology vol. 1, Wiley-vch Berlin, 2008.
[4] R.W. Solarz, Laser Spectroscopy and its Applications, Routledge, 2017.
[5] F. Ceballos, H. Zhao, Ultrafast laser spectroscopy of two-dimensional materials beyond graphene, Adv. Funct. Mater. 27 (2017) 1604509.
[6] R. Sroka, H. Stepp, G. Hennig, G.M. Brittenham, A. Rühm, L. Lilge, Medical laser application: translation into the clinics, J. Biomed. Optic. 20 (2015) 061110.
[7] D. Paul, L.M. Robeson, Polymer nanotechnology: nanocomposites, Polymer 49 (2008) 3187–3204.
[8] A. Yogo, K. Sato, M. Nishikino, M. Mori, T. Teshima, H. Numasaki, M. Murakami, Y. Demizu, S. Akagi, S. Nagayama, Application of laser-accelerated protons to the demonstration of DNA double-strand breaks in human cancer cells, Appl. Phys. Lett. 94 (2009) 181502.
[9] E. Murphy, The semiconductor laser: enabling optical communication, Nat. Photon. 4 (2010) 287.
[10] P. Corrigan, R. Martini, E.A. Whittaker, C. Bethea, Quantum cascade lasers and the kruse model in free space optical communication, Optic Express 17 (2009) 4355–4359.
[11] L. Zang, Y. Che, J.S. Moore, One-dimensional self-assembly of planar π-conjugated molecules: adaptable building blocks for organic nanodevices, Acc. Chem. Res. 41 (2008) 1596–1608.
[12] G. Barbarella, M. Zangoli, F. Di Maria, Synthesis and applications of thiophene derivatives as organic materials, Advances in Heterocyclic Chemistry, vol. 123, Elsevier, 2017, pp. 105–167.
[13] R. Gupta, M. Stevenson, A. Dogariu, M. McGehee, J. Park, V. Srdanov, A. Heeger, H. Wang, Low-threshold amplified spontaneous emission in blends of conjugated polymers, Appl. Phys. Lett. 73 (1998) 3492–3494.
[14] G. Heliotis, R. Xia, D. Bradley, G. Turnbull, I. Samuel, P. Andrew, W.L. Barnes, Blue, surface-emitting, distributed feedback polyfluorene lasers, Appl. Phys. Lett. 83 (2003) 2118–2120.
[15] E. Choi, L. Mazur, L. Mager, M. Gwon, D. Pitrat, J. Mulatier, C. Monnereau, A. Fort, A. Attias, K. Dorkenoo, Photophysical, amplified spontaneous emission and charge transport properties of oligofluorene derivatives in thin films, Phys. Chem. Chem. Phys. 16 (2014) 16941–16956.

[16] Y. Lin, X. Zhan, Oligomer molecules for efficient organic photovoltaics, Acc. Chem. Res. 49 (2015) 175–183.
[17] M. Nagawa, R. Hibino, S. Hotta, H. Yanagi, M. Ichikawa, T. Koyama, Y. Taniguchi, Emission gain narrowing from single crystals of a thiophene/phenylene co-oligomer, Appl. Phys. Lett. 80 (2002) 544–546.
[18] R. Ho-Wu, K. Sun, T. Goodson III, Synthesis and enhanced linear and nonlinear optical properties of chromophore–au metal cluster oligomers, J. Phys. Chem. C 122 (2018) 2315–2329.
[19] D. Pisignano, M. Anni, G. Gigli, R. Cingolani, M. Zavelani-Rossi, G. Lanzani, G. Barbarella, L. Favaretto, Amplified spontaneous emission and efficient tunable laser emission from a substituted thiophene-based oligomer, Appl. Phys. Lett. 81 (2002) 3534–3536.
[20] Y. Tanaka, K. Goto, K. Yamashita, T. Yamao, S. Hotta, F. Sasaki, H. Yanagi, Vertical cavity lasing from melt-grown crystals of cyano-substituted thiophene/phenylene co-oligomer, Appl. Phys. Lett. 107 (2015) 100_101.
[21] M.S. AlSalhi, A.R. Almotiri, S. Prasad, M.J. Aljaafreh, A.H. Othman, V. Masilamai, A temperature-tunable thiophene polymer laser, Polymers 10 (2018) 470.
[22] G. Turnbull, P. Andrew, M. Jory, W.L. Barnes, I. Samuel, Relationship between photonic band structure and emission characteristics of a polymer distributed feedback laser, Phys. Rev. B 64 (2001) 125122.
[23] D. Fichou, S. Delysse, J.M. Nunzi, First evidence of stimulated emission from a monolithic organic single crystal: A-octithiophene, Adv. Mater. 9 (1997) 1178–1181.
[24] S. Prasad, K. Ibnaouf, M. AlSalhi, D. Devaraj, V. Masilamani, High power amplified spontaneous emission from an oligomer in solution, J. Lumin. 168 (2015) 109–113.
[25] D. Moses, High quantum efficiency luminescence from a conducting polymer in solution: a novel polymer laser dye, Appl. Phys. Lett. 60 (1992) 3215–3216.
[26] S. Abdulaziz Alfahd, S. Prasad Rajendra, W. Al-Mujammi, D. Devaraj, V. Masilamani, M.S. AlSalhi, An efficient violet amplified spontaneous emission (ase) from a conjugated polymer (pfo-co-px) in solution, Materials 10 (2017) 265.
[27] M. Ichikawa, K. Nakamura, M. Inoue, H. Mishima, T. Haritani, R. Hibino, T. Koyama, Y. Taniguchi, Photopumped laser oscillation and charge-injected luminescence from organic semiconductor single crystals of a thiophene/phenylene co-oligomer, Appl. Phys. Lett. 87 (2005) 221113.
[28] H. Mizuno, T. Maeda, H. Yanagi, H. Katsuki, M. Aresti, F. Quochi, M. Saba, A. Mura, G. Bongiovanni, F. Sasaki, Optically pumped lasing from single crystals of a cyano-substituted thiophene/phenylene co-oligomer, Advanced Optical Materials 2 (2014) 529–534.
[29] H. Yanagi, K. Tamura, Y. Tanaka, F. Sasaki, Optically pumped lasing from single-crystal cavity of p-phenylene oligomer, Adv. Nat. Sci. Nanosci. Nanotechnol. 5 (2014) 045013.
[30] F. Kong, J. Liu, X. Zhang, Y. An, X. Li, B. Lin, T. Qiu, Effect of distance between acceptor and donor on optical properties of composite semiconducting polymer films, J. Lumin. 131 (2011) 815–819.
[31] T. Virgili, D.G. Lidzey, D.D. Bradley, Efficient energy transfer from blue to red in tetraphenylporphyrin-doped poly (9, 9-dioctylfluorene) light-emitting diodes, Adv. Mater. 12 (2000) 58–62.
[32] A. Mallick, B. Haldar, S. Sengupta, N. Chattopadhyay, 7-hydroxy-4-methyl-8-(4′-methylpiperazine-1′-yl) methyl coumarin: an efficient probe for fluorescence resonance energy transfer to a bioactive indoloquinolizine system, J. Lumin. 118 (2006) 165–172.
[33] S. Azim, H. El-Daly, S. El-Daly, K.A. Abou-Zeid, E. Ebeid, J. Heldt, Energy transfer and photodecomposition of antharacene laser dyes, J. Chem. Soc., Faraday Trans. 92 (1996) 2685–2688.
[34] F. Reil, U. Hohenester, J.R. Krenn, A. Leitner, Forster-type resonant energy transfer influenced by metal nanoparticles, Nano Lett. 8 (2008) 4128–4133.
[35] J. Zheng, Spectroscopy-based quantitative fluorescence resonance energy transfer analysis, Ion Channels, Springer, 2006, pp. 65–77.
[36] B.A. Al-Asbahi, M.H.H. Jumali, C.C. Yap, M.M. Salleh, M.S. AlSalhi, Inhibition of dark quenching by tio2 nanoparticles content in novel pfo/fluorol 7ga hybrid: a new role to improve oled performance, Chem. Phys. Lett. 570 (2013) 109–112.
[37] L. Gartzia-Rivero, L. Cerdán, J. Bañuelos, E. Enciso, I.n.i. López Arbeloa, A.n. Costela, I. García-Moreno, Förster resonance energy transfer and laser efficiency in colloidal suspensions of dye-doped nanoparticles: concentration effects, J. Phys. Chem. C 118 (2014) 13107–13117.
[38] S. Chen, H. Chou, A. Su, S. Chen, Molecular packing in crystalline poly (9, 9-di-n-octyl-2, 7-fluorene), Macromolecules 37 (2004) 6833–6838.
[39] W.M. Mujamammi, S. Prasad, M. Saleh AlSalhi, V. Masilamani, Time evolution of the excimer state of a conjugated polymer laser, Polymers 9 (2017) 648.
[40] T. Forster, Delocalized excitation and excitation transfer, in: O. Sinaoglu (Ed.), Modern Quantum Chemistry, vol. 3, Academic Press, New York, 1965, pp. 93–137.
[41] R.M. Clegg, Förster resonance energy transfer—fret what is it, why do it, and how it's done, Lab. Tech. Biochem. Mol. Biol. 33 (2009) 1–57.
[42] D. O'Carroll, D. Iacopino, A. O'Riordan, P. Lovera, É. O'Connor, G.A. O'Brien, G. Redmond, Poly (9, 9-dioctylfluorene) nanowires with pronounced β-phase morphology: synthesis, characterization, and optical properties, Adv. Mater. 20 (2008) 42–48.
[43] T. Komori, H. Nakanotani, T. Yasuda, C. Adachi, Light-emitting organic field-effect transistors based on highly luminescent single crystals of thiophene/phenylene co-oligomers, J. Mater. Chem. C 2 (2014) 4918–4921.
[44] P.R. Selvin, [13] fluorescence resonance energy transfer, Methods in Enzymology, vol. 246, Elsevier, 1995, pp. 300–334.
[45] D. Zhang, M. Cai, Y. Zhang, Z. Bin, D. Zhang, L. Duan, Simultaneous enhancement of efficiency and stability of phosphorescent oleds based on efficient forster energy transfer from interface exciplex, ACS Appl. Mater. Interfaces 8 (2016) 3825–3832.
[46] J.R. Lakowicz, Energy transfer, Principles of Fluorescence Spectroscopy, Springer, 1999, pp. 367–394.